

GENERALIZED MÖBIUS-LISTING BODIES AND THE HEART

J. GIELIS, I. TAVKHELIDZE AND P.E. RICCI

ABSTRACT. Generalized Möbius-Listing surfaces and bodies generalize Möbius bands, and this research was motivated originally by solutions of boundary value problems. Analogous to cutting of the original Möbius band, for this class of surfaces and bodies, results have been obtained when cutting such bodies or surfaces. The results can be applied in a wide range of fields in the natural science, and here we propose how they can serve as a model for the heart and the circulatory system.

Mathematics Subject Classification (2010): 37N25, 53A05, 57M25, 92C42

Key words: GML bodies, Heart, Möbius

Article history:

Received: November 5, 2023

Received in revised form: November 13, 2023

Accepted: November 15, 2023

1. INTRODUCTION

The classical Möbius band can be realized by sweeping a line piece along a circle as central basic line, and perpendicular to this basic line; moreover, the basic line cuts the piece of line exactly in the middle (Figure 1a). Figure 1 shows how a ribbon can be connected, with an odd or even number of twists (the upper index). In the case the number of twists is odd, the surface is called non-orientable, and the surface is one-sided; in other words, a traveler moving on the Möbius band will return at his or her original position and will have visited all parts of the ribbon (“Möbius condition”). In contrast, when the number of twists is even, then the surfaces will be like a cylinder, with an inner and an outer surface (“Cylinder condition”). A traveller starting on one side will return on the same side, and not see the other side. A Möbius band can be painted with a single color, for a cylinder, two colors are needed.

Generalized Möbius-Listing surfaces and bodies (*GML*) generalize the Möbius band or ribbon in a geometrical way: both the basic line and the cross section can be chosen from a wide range of shapes. Instead of starting from a ribbon, *GML*'s start from prisms (or cylinders), of which the two ends are connected. The notation is GML_m^n and in this sense Figures 1a-d have $m = 2$, hence the notation GML_2^n . When $n = \text{even}$, the shapes have cylinder condition, and when $n = \text{odd}$, the shapes exhibit the Möbius condition [31], [37]. In a recent article, these shapes have been called the Möbius helicoid (isometric to a linear helicoid) and have been related to masses of elementary particles and to the Lorentz factor by the number of twists. The Möbius band provides for the natural phase space for fermionic fields, whereas the cylinder provides this for bosonic fields [19]. Möbius bands are also very common in chemistry [21], [30].

These, however, are only the simplest of possibilities. Both the path and the cross section that is swept along the path can be extended to include polygons, rose curves and Gielis curves, and the end points need not be connected. In Section 2 Generalized Möbius-Listing surfaces are defined, which are closed figures. One can image a prism with a certain cross section, of which the two ends are joined. They are a subset of Generalized Twisting and Rotating Surfaces and Bodies GTR_m^n , which are in general open structures. In Section 3 and 4 some main results of cutting GML_m^n surfaces and bodies are recalled, and in Section 5 the conditions under which a Link-1 single body with Möbius phenomenon is obtained

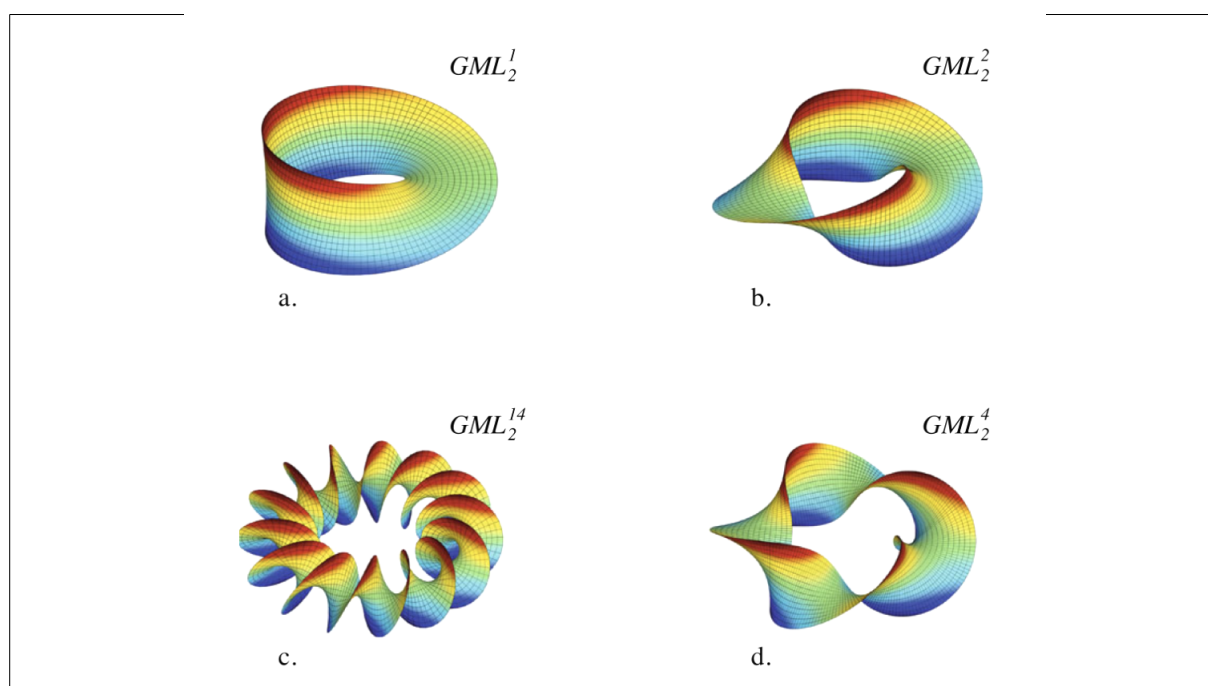


FIGURE 1. Ribbons with twists before joining. Case a. is the classic Möbius strip.

after cutting, are defined. Since the analytic definitions of GML_m^n surfaces and bodies allow for dynamic changes, the question arose how much of the whole body needs to have the specific conditions to obtain the results after cutting. As shown in Section 6, it turns out that only one cross section is needed with the right conditions, and several examples are given. Finally in Section 7 we explain how the heart is a GML_m^n body, and we propose that this can be extended to the whole circulatory system. The dynamics of the heart and the whole system can then be considered as a switching between cylinder and Möbius conditions.

2. GENERALIZED MÖBIUS LISTING SURFACES AND BODIES

Generalized Möbius-Listing Bodies GML_m^n are defined analytically by Equation (2.1) [35]:

$$\begin{cases} X(\tau, \psi, \theta, t) = T_1(t) + [R(\theta, t) + p(\tau, \psi, \theta, t) \cos(\psi + \frac{n\theta}{m})] \cos(\theta + M(t)) \\ Y(\tau, \psi, \theta, t) = T_2(t) + [R(\theta, t) + p(\tau, \psi, \theta, t) \cos(\psi + \frac{n\theta}{m})] \sin(\theta + M(t)) \\ Z(\tau, \psi, \theta, t) = T_3(t) + Q(\theta, t) + p(\tau, \psi, \theta, t) \sin(\psi + \frac{n\theta}{m}) \end{cases} \quad (2.1)$$

X, Y, Z, t is the ordinary notation for space and time coordinates and τ, ψ, θ are local coordinates where $\tau \in [-\tau^*, \tau^*]$, with $0 < \tau; \psi \in [0; 2\pi]$ and $\vartheta \in [0; 2\pi h]$, with $h \in \mathbb{R}$. The functions $T_{1,2,3}(t), R(\psi, \theta, t), p(\tau, \psi, \theta, t), M(t)$ and $Q(\theta, t)$, as well as parameter $\mu = \frac{n}{m}$, define simple movements.

Definition 2.1. The basic line of a GML_m^n body is the continuous closed, generally spatial curve, generated by the center of the prism in its movement necessary to obtain, after n twists, the joining of the two opposite faces of the prism. This basic line can be a circle P_∞ (and any curve homeomorphic to a circle) or a self-intersecting curve like a Pascal’s limaçon, which closes after two full rotations. The basic line can also be other planar or space curves, for example, Gielis curves [8], [24], [11], or Grandi

(rose) curves $\rho = \cos m\theta$ [33]. In this general case the notation $GML_m^n(v)$ is used with $v \in \mathbb{Q}$ denoting the shape of the basic line, with $v = 1$ if the basic line is a circle.

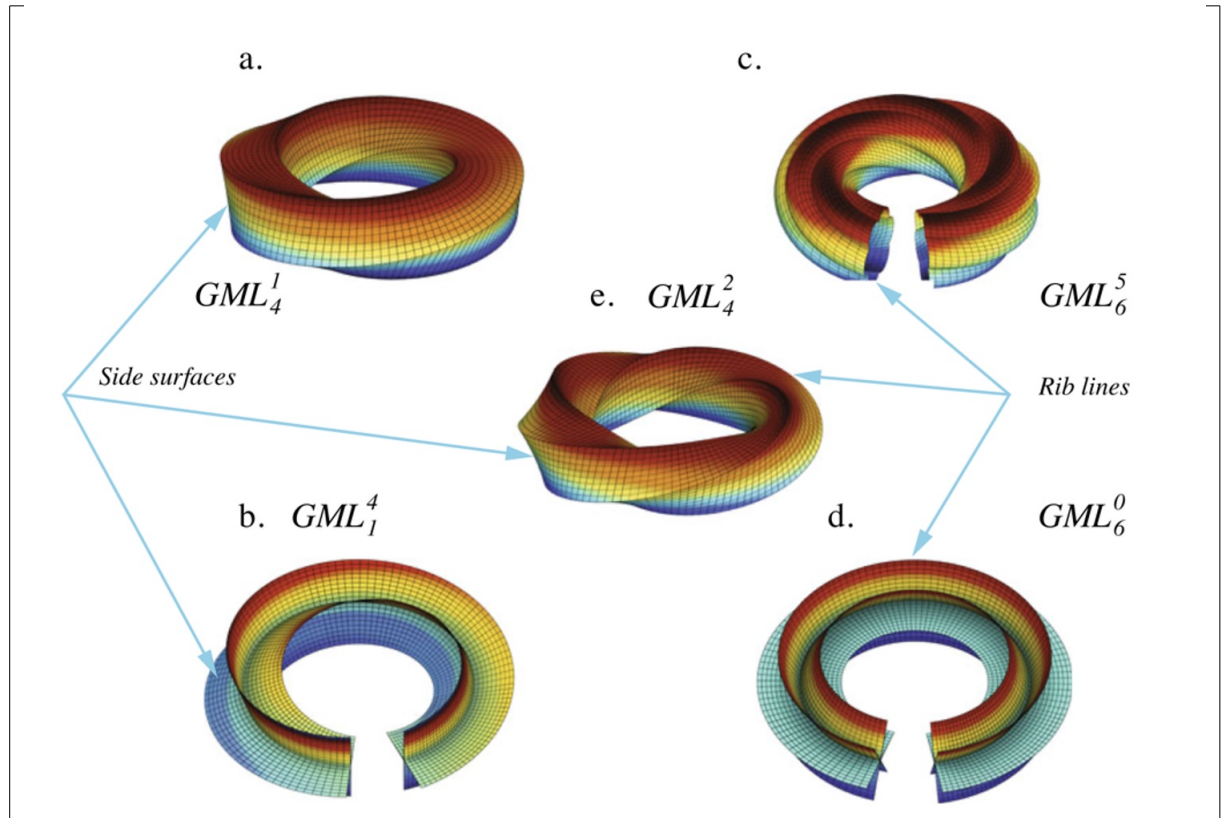


FIGURE 2. (a-e) Identification of vertices, with twists leading to GML_m^n .

Definition 2.2. The twisting parameter $\mu = \frac{n}{m}$ describes the characteristic of twisting where m is the number of vertices of the regular polygon P_m (the shape of the radial cross section) and n is the number of twisting of the cross section of the prism before identification of its ends. If $\mu = \frac{n}{m}$ is an integer number ($n = km$), then the corresponding lines makes k coils after one rotation around the torus. If $\frac{n}{m} \in \mathbb{Q}$ then the corresponding line makes n coils after m rotations around the torus. If $\frac{n}{m} \in \mathbb{R} \setminus \mathbb{Q}$ then the line makes infinite coils after infinite rotations around the torus without self-intersections.

Definition 2.3. A rib of the $GML_m^n(v)$ for each $v \in \mathbb{Q}$, is a continuous closed, in the general case, spatial line on which are situated only the vertices of the radial cross section of this body (i.e., the torus line with characteristic $\frac{n}{m}$). Between the ribs, planes or curved surfaces can be spanned giving rise to a GML_m^n side surfaces (Figure 2), and if the whole structure is solid (i.e., all cross sections are disks), then one obtains GML_m^n bodies.

Obviously one can also define shell structures, by limiting the radial function of the cross sections. GML_m^n bodies and surfaces are always closed, hence they are a subset of closed Generalized Twisting and Rotating bodies GTR_m^n [35]. In this general, case the ends of the prims need not be closed, and the basic line can be a spiral, a helix or any 3D curve.

The original motivation to study GML_m^n surfaces and bodies is that the solution of boundary value problems for partial differential equations is easier to obtain with direct knowledge of the domain, and

with the extension of surfaces to bodies, also of the internal geometry and connected domains inside GML_m^n bodies. It allows for understanding the precise relation between the asymptotic behavior of solutions and the geometrical structure of boundary [35]. GML surfaces generalize a wide range of 3D surfaces, including implicit, tube and canal surfaces [1], [5], and twisted structures [17]. They provide for a generic model for strings (see [26]), but in contrast to strings, GML bodies and surfaces are not elementary, since they can be cut, however small the size.

3. THE CUTTING PROBLEM

Definition 3.1. Cutting of a GML_m^n body with a regular polygon as cross section is performed with (1) a straight knife, which (2) cuts perpendicular to the polygonal cross section of the surfaces and bodies, and (3) the knife cuts the m -polygon boundary exactly in two points or two times (depending on the thickness of the knife). For (3) there are three possibilities: the cut of the polygon can be from a vertex to a vertex VV , from a vertex to a side or edge VS , or from side to side SS (=edge to edge). The precise orientation of this knife (and the positions where it cuts the boundary) is maintained during the complete cutting process, until the knife returns to its starting position, and the cutting is completed.

The point of the knife traces out a toroidal line along the body or surface. In general, cutting leads to separate bodies or surfaces, but in particular cases, a single body results, similar to the single surface that results from cutting the original Möbius band along the basic line. In most cases very complex structures are obtained [32], [39]. Figure 3 shows the result of cutting a pentagonal GML from side 1 to side 3, below center [39]. The result is three different bodies, (triangular, quadrangular, and pentagonal), linked together as a Link-3 object. Each of these objects has a certain number of twists and the structures can be knot-like. Such structures have been observed in quantum chemistry [20].

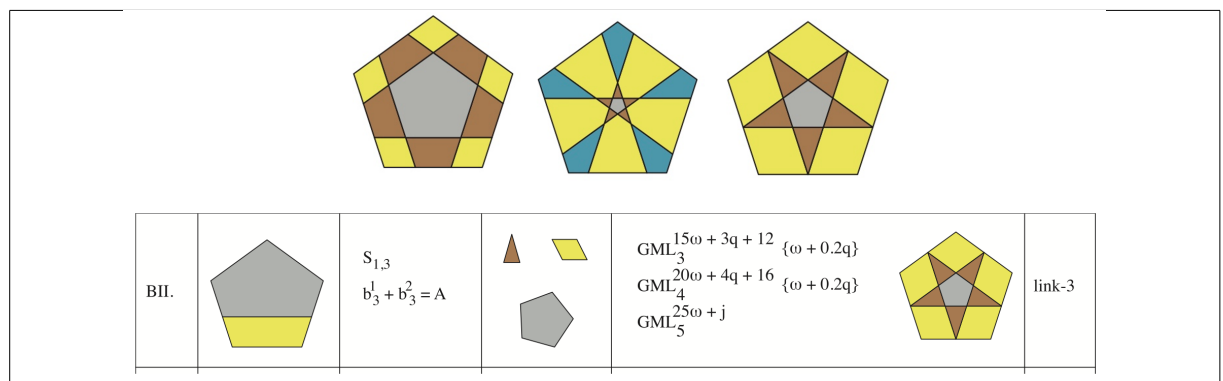


FIGURE 3. Three different ways of cutting a pentagon side to side. Below: Case BII, $S_{1,3}$ and the different outcomes connected via Link-3.

In analogy with the cutting of a classic Möbius band along the central line, we define the Möbius phenomenon as follows:

Definition 3.2. The Möbius phenomenon occurs when, after cutting of a GML_m^n body or surface, a single body or surface results, where one can travel along a rib or a side surface and return to the original position.

Cutting the Möbius band along the basic line, yields a single surface. If it is cut along any other straight line, the result is a link of two different surfaces. The second author generalized this result for any n and m , and for any number of knives [32]. When dealing with GML surfaces and bodies, more objects can result after cutting. Depending on where precisely the knife cuts (through the centre of the

polygon or not; from vertex to vertex; from side to side, or from vertex to side), and on the cross section and the number of twists of the GML_m^n many different outcomes result [35]. In Figure 3 three different results of $SS_{1,3}$ cuts are shown, with two cases of Link-3 (three bodies) and one case of Link 4 (four bodies). The only difference is the particular spot on the sides where cuts are made.

Shapes of radial cross sections $GML_4^{4\omega}$	Cut	Parameters of the objects which appear after cutting					
		Shapes of radial cross sections	Structure of elements	Link group of elements	Link group of object		
A.	$SS_{1,2}$		$GML_5^{5\omega}$ $GML_3^{3\omega}\{\omega\}$	Link-1	Link-2		
B. a.	$SS_{1,3}$		$GML_4^{4\omega}$ $GML_4^{4\omega}\{\omega\}$				
B. b.	$S_{1,3,C}$		$GML_4^{4\omega}\{\omega\}$ $GML_4^{4\omega}\{\omega\}$				
C.	$VS_{1,2}$		$GML_4^{4\omega}$ $GML_3^{3\omega}\{\omega\}$			$\{0_1\}$	$\{(2\omega)_1^2\}$
D.	$VV_{1,3}$		$GML_3^{3\omega}\{\omega\}$ $GML_3^{3\omega}\{\omega\}$				

Shapes of radial cross sections $GML_4^{4\omega+2}$	Cut	Parameters of the objects which appear after cutting			
		Shapes of radial cross sections	Structure of elements	Link group of elements	Link group of object
A.	$SS_{1,2}$		$GML_6^{6\omega+3}$ $GML_3^{6\omega+6}\{\omega+0.5\}$	Link-2	Link-2
B.I	$SS_{1,3}$		$GML_4^{4\omega+2}$ $GML_4^{8\omega+8}\{\omega+0.5\}$		
B.II	$SS_{1,3,C}$		$GML_4^{8\omega+8}\{\omega+0.5\}$	Link-1	Link-1
C.	$VS_{1,2}$		$GML_4^{4\omega+2}$ $GML_3^{6\omega+6}\{\omega+0.5\}$	Link-2	Link-2
D.	$VV_{1,3}$		$GML_3^{6\omega+6}\{\omega+0.5\}$	Link-1	Link-1

FIGURE 4. Cutting of GML_4^n bodies, without (left) or with twist (right).

After cutting very complex structures can result, but under certain conditions, a single body will result. Figure 4 shows all possible results after cutting of an untwisted and a twisted square torus. Here $SS_{1,2}$ and $S_{1,3}$ indicate that the knife cuts from side 1 to sides 2 and 3 respectively. Likewise, VS stands for vertex-to-side cuts and VV for vertex-to-vertex cuts. In case B and D (Figure 4 left), the cut is through the center) of a GML body with square cross sections; the result is always two bodies. In case BII and D (Figure 4 right) with cut through the center of a GML body with square cross section, the result is always a single body, denoted by Link-1. The results have been classified for lower symmetries ($m = 2, 3, 4, 5, 6$) [35], [32], [36], [15], [6]. The results of cutting GML for the general case have been reported in [12], in Theorems 3.3 and 3.4.

Theorem 3.3. *The geometrical solution. The total number of different ways of cutting an m -polygon Ξ_m^{geo} is the number of 1 or m cuts, times the number of divisors of m .*

- (1) For even $m (= 2k)$: $\Xi_m^{geo} = N_m^{div} (m + 1 + N_{m-2}^{SS})$
- (2) For odd $m (= 2k + 1)$: $\Xi_m^{geo} = N_m^{div} (m + 2 + N_{m-2}^{SS})$

Theorem 3.4. *The topological solution*

- (1) If $m = 2k + 1$ and has N nontrivial divisors $d_2, d_3 \dots d_{N+1}$ and $d_1 \equiv 1, d_{N+2} \equiv d_m \equiv m$, then the number of all possible variants of cutting of GML_m^n bodies is $\Xi_m^{top} = 8k + 1 + 3Nk + \sum_{i=2}^{N+1} \left\lfloor \frac{k}{d_i} \right\rfloor + 2N$
- (2) If $m = 2k$ and has N nontrivial divisors $d_2, d_3 \dots d_{N+1}$ and $d_1 \equiv 1, d_{N+2} \equiv d_m \equiv m$, then the number of all possible variants of cutting of GML_m^n bodies is $\Xi_m^{top} = 8k - 5 + 3Nk + \sum_{i=2}^{N+1} \left\lfloor \frac{k-1}{d_i} \right\rfloor - N$

Remark 3.5. The topological solution is a slightly different form compared to Th 3.3: $\sum_{all\ div} (N_{m=2k}) = \Xi_m^{top}$ depending on whether the total number of variants is expressed in terms of total number of divisors or total number of non-trivial divisors N (excluding d_1 and d_m). The proof of Theorem 3.4 is based on the fundamental facts from the theory of cyclic groups with a finite number of elements (m);

- (1) The number of cyclic subgroups is the number (N) of nontrivial divisors of m .
- (2) The number of elements in each subgroup is the number of transactions and equal to the $gcd(m, i)$
- (3) The number of cuts is either 3 or 1, (3 or 1 mod 8) and this is determined by the property of the subgroup and the property of the cut line – i.e. when the number of cuts is three, then the ends of the survey line lie on the same strings of the initial polygon, except for the case when $k = [m/2] + 1$
- (4) If $k = [m/2] + 1$, and for an odd number m the number of cuts is 5, and for even m the number of cuts is 2. This is determined by the property of the subgroup and the property of the cut line. In the latter case $m = 2k$ an important role is played by the rotational symmetry.

Remark 3.6. Ongoing research focuses on defining the exact shapes resulting from cutting, see [34], [38].

4. 3-D BODIES AND 2-D CROSS SECTIONS WITH R-FUNCTIONS

Theorems were derived after the problem of cutting of 3D *GML* surfaces and bodies could be reduced to a problem of planar geometry, whereby the results depend only on the cross section $p(\tau, \psi, t)$ and the twisting parameter μ . The self-intersecting curves for any rational m , lead to various sectors in the polygons or cross sections of the *GML* body. In Figure 3 the Link-3 cases have three zones, while the Link-4 case has four different zones of different shapes indicated with 4 different colors. In *GML* bodies, when cut and separated, these zones represent different bodies of 3D *GML* surfaces and bodies.

For rational $m = p/q$, the number of zones created is determined by q , and the symmetry of the polygons/polygrams is determined by p . In Figure 5 Left panel, five different layers or zones can be defined in different shades of blue. Layers L_0 to L_4 are defined as a combination of layers from inside to outside and all layers have 7 maxima and 7 minima. A ray drawn from the center 0 in any direction has multiple values indicated by I_0 to I_4 (red dots). When rotating the ray around the centre, the values of I_0 define the boundaries of L_0 and the ray then sweeps the full area of L_0 . Values of I_0 and I_1 define the boundaries of L_1 , and here I_0 and I_1 coincide at maxima for L_0 and at minima for L_1 . In the same way, values of I_i and I_{i+1} define layer L_{i+1} .

In this way zones can be defined, not only as stacked layers L in Figure 5a, but as separate layers or combinations of layers. We define l_i as separate zones based on the different hues of blue zones in $L_{0,\dots,4}$ in Figure 5 left panel. Examples of separate zones or combinations are given in Figure 4b; clockwise, from upper left (with $L_0 = l_0$) [7]:

- (1) $l_1 = L_1 - L_0$
- (2) $l_2 = L_2 - L_1$
- (3) $l_3 = L_3 - L_2$
- (4) $l_1 + l_2 = L_2 - L_0$

The zones and the independent domains separated by lines correspond to self-intersecting curves. These independent figures can be connected into layers or zones (Figure 5a,b) using *R*-functions [12],[7]. Basic Boolean operations can be used to define the different layers and separate sectors like those in Figure 5, and these can be translated into geometric language, using *R*-functions, whereby the different layers or different sectors are defined as single geometrical domains or combinations of single domains. One of the most commonly used *R*-functions are \mathfrak{R}_p functions, defined by $|x_1|^p + |x_2|^p \pm [|x_1|^p + |x_2|^p]^{\frac{1}{p}}$, with + and - denoting conjunction and disjunction. Hence separated regions in 2D cross sections of *GML* in general can be defined as coherent structures, completely in line with the fact that in 3D the structures are indeed coherent.

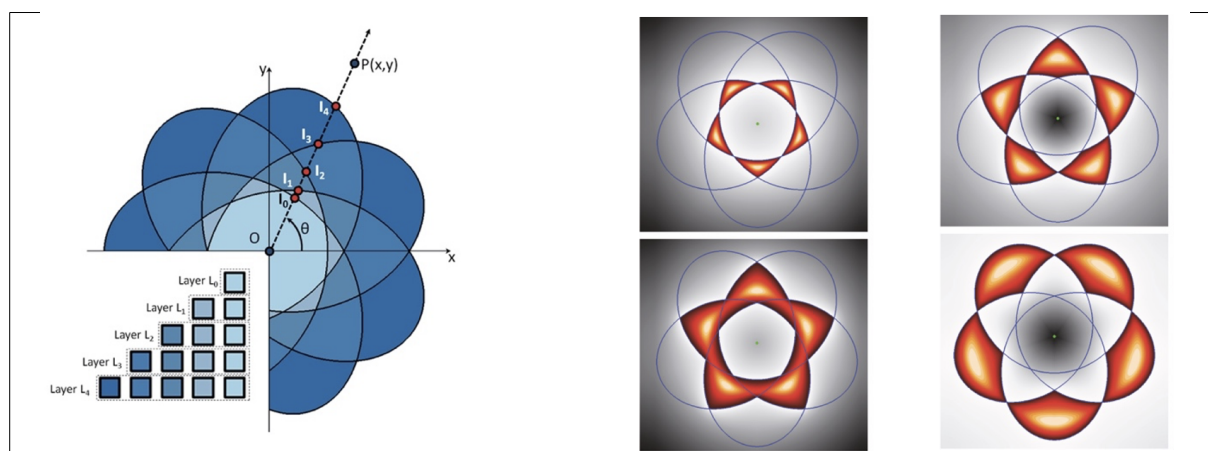


FIGURE 5. Left: Different layers in Rational Gielis curves RGC. Right: RGC for $p = 5$ and $q = 4$ with different zones defined [7].

Remark 4.1. The process of cutting does not necessarily lead to the different substructures falling apart. One can think of various physical process that creates different domains without separation, such as torsion or vibration [12], [14]. Furthermore, if the cross section of the prism is a rose curve, then the process of connecting two ends of the prisms leads to single or multiple hollow bodies or tubing systems, depending on the twisting [33].

Remark 4.2. R -functions are not restricted to Boolean operations, but can be extended to n -valued logics and n partitions of space [29]. Examples of extensions of R -functions to 3-valued logics are found in [9], [18].

5. LINK-1 WITH MÖBIUS PHENOMENON AFTER CUTTING

Under certain conditions cutting of twisted GML 's, can yield a single body (Link-1). It happens when the cut is through the centre (cases BII and D in Figure 4b). With the process of cutting described above, with a knife cutting from side to side, vertex to vertex or side to vertex, it turned out that a single body could only be obtained for polygons with an even number of vertices and edges, and only when the cut was through the centre (cases BII and D in Figure 4b). The knife used in this cutting is called a chordal knife, since it cuts the polygon in precisely two points.

Theorem 5.1. *In the cutting of GML bodies with chordal knives, the Möbius phenomenon with one resulting body and link number Link-1 can appear only for m even and when the knife cuts through the centre.*

Using a radial knife on the other hand cuts the polygon in precisely one point and then the Möbius phenomenon can be obtained for $m = \text{odd}$ and $m = \text{even}$, odd and even polygons, respectively [13].

Theorem 5.2. *In the cutting of GML bodies the Möbius phenomenon can appear for both m odd and m , when the knife is a radial knife, a ray starting at the centre of the polygon.*

Remark 5.3. A chordal knife is named after a chord, defining the trigonometric functions on a circle. A radial knife starting in the center is the position vector. This acts as the hand of a clock with discrete ticks (Figure 6) but with continuous movement within a GML_m^n body, keeping a fixed direction from center to the vertex. The tip of the position vector traces out a toroidal line, wound around the torus, now in a continuous way.

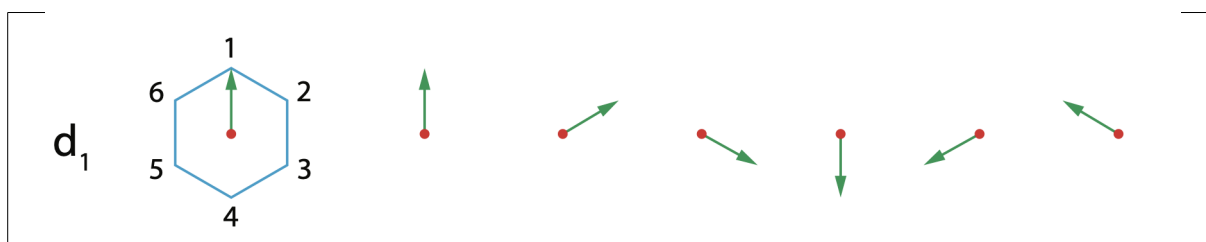


FIGURE 6. Radial knife or position vector

6. A SINGLE CROSS SECTION WITH THE RIGHT SYMMETRY SUFFICES

The cross section of the GML_m^n is generally assumed to be constant along the whole structure, whereas Equation (2.1) allows for a changing cross section along the GML_m^n . A direct example of a GML_m^n body with changing cross section is when the cross sections change along the body. These changes can occur smoothly or in discrete jumps. Equation (2.1) includes a time variable t , important if the GML_m^n body represents any physical or biological system. The question then is whether all cross sections have to retain the condition of rotational symmetry, to achieve the Link-1 or Möbius phenomenon. Will a Link-1 structure still occur if the cross sections of the GML_m^n change from the starting point, where the conditions are met, to an intermediate section that does not meet these conditions, and again close with the original cross section? The answer is:

Theorem 6.1. [16] *In the cutting of GML_m^n bodies under the above conditions (radial knife cutting through the center for both odd and even regular polygons, or chordal knife cutting through the center for even regular polygons) a sufficient condition is that only one cross section is rotationally symmetric, to obtain the Link – 1 result with the Möbius phenomenon.*

Proof. The cross sections at the start and end of the GML_m^n body are the same. If cross sections are denoted as $S_0, S_1, S_2, \dots, S_q$, then the set of all cross sections is denoted as $]S_0, S_1, S_2, \dots, S_q[$. The sequence of cross sections can be continuous for $q \rightarrow \infty$, discrete for $q < \infty$, or partially discrete, partially continuous. The condition for a smooth joint of both ends is when $S_0 = S_q$. Additionally the orientation of both is twisted before joining (e.g. 180° in the case of a square), denoted as $\uparrow S_0 = \downarrow S_q$. For cutting, one can assume the same, constant shape along the whole GML_m^n bodies, so that the knife follows the classical toroidal lines (ribs or slit surfaces). In this case only S_0 and S_q are relevant, but not $]S_1, S_2, \dots, S_{q-1}[$, and the cutting then reduces to the general case of cutting GML_m^n bodies. \square

Remark 6.2. For the proof of Theorem 6.1 a simplified version can be used, since only the cross section $p(\tau, \psi)$ and the twisting parameter n , are involved.

Remark 6.3. Since one can always find a way of cutting (or division of zones) whereby at the end of the day, the whole shape turns out to be a one-sided body, coherent in any sense of the word. As long as one cross section fulfills the conditions, all other cross sections $]S_1, S_2, \dots, S_{q-1}[$ may be anything.

Example 6.4. [16] The cross sections $]S_1, S_2, \dots, S_{q-1}[$ may consist of dispersed data points, distributed according to some probability (density) function or randomly (maximum entropy). As long as the cut is executed correctly, the result will be a single body (Link-1), displaying the Möbius phenomenon of one-sidedness.

Example 6.5. [16] Figure 7 shows a GML_4^n structure connected to a brane [15]. Since the two sections at the brane are the same, namely $S_0 \equiv S_q$, one can define the cutting process in such a way that, whatever goes in comes out the same on the other side, so that everything remains connected as a Link-1 irrespective of what happens inside the GML -wormhole.

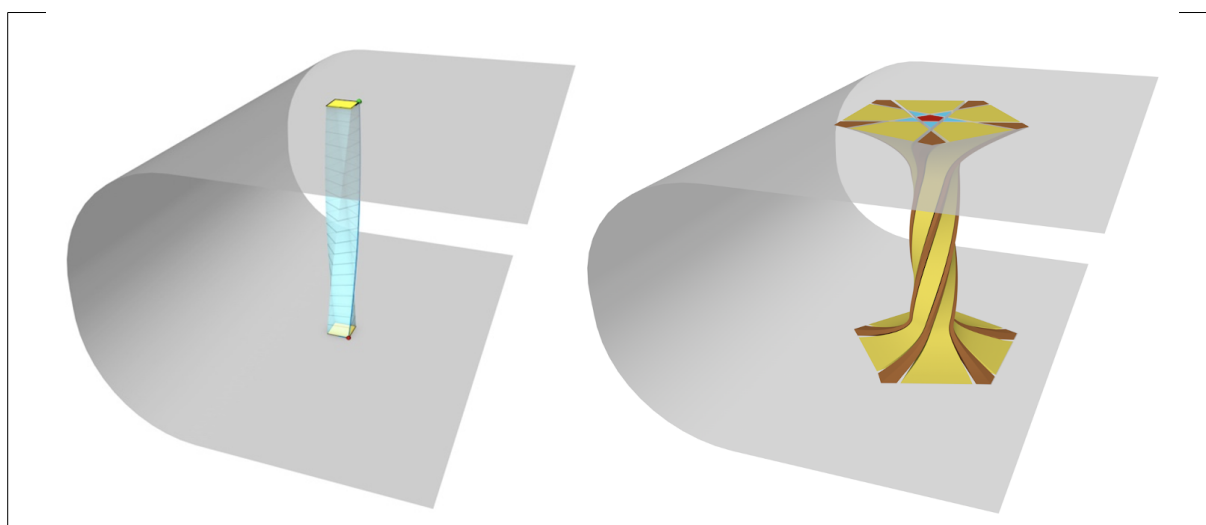


FIGURE 7. Partial or complete GML bodies, with cross sections on brane [12]

Example 6.6. A tubing system with cross section S_0 that branches out into various ever smaller tubes; then the smaller tubes rejoin into larger tubes, to end up with the original tube size at S_q . Such branching may conserve area at every stage. One example is the branching in the circulatory system, with main vessels (Aorta, Superior and Inferior Vena Cava and pulmonary arteries and veins), arteries, arterioles and capillaries) [43].

The circulatory system has evolved with physical separation of transport and exchange, with transport from the heart to lungs and the body via main veins and arteries, and exchange via the capillaries and the alveoli in lungs. In the latter case the capillaries and alveoli are porous for exchange of gases, creating the possibility for a single sided surface.

Proposition 6.7. *The branching of the circulatory closed or open system can be partially transport and partially exchange.*

In the first case we have a partial tubing system, where the system of tubes has an outside and an inside, analogous to a torus and *Transport* is key function. In the second case, inside and outside are connected via pores and oxygen and carbon dioxide can flow in and out of the cells into the tubing systems (and in reverse order in the lungs). *Exchange* is the key function. Beyond the physical separation, the dynamics of the heart and the circulatory system may be understood as switching between transport and exchange.

7. SWITCHING BETWEEN CYLINDER AND MÖBIUS CONDITION

The heart evolved from a tubular open structure to a circulatory system, with every increasing complexity [2], [22]. As tubular structures the main action to move fluids is via peristaltic movement. Such structures can be modeled as *GTR* bodies, for primitive open structures, or as *GML* bodies for closed circulatory systems. The original circulatory tubular system later evolved into folded structures, creating the heart characteristic of higher animals (mammals, fish, reptiles, amphibians), with different chambers and valves.

The Spanish cardiologist Torrent-Guasp considered the heart as a helical structure, based on the study of one thousand hearts of humans, various mammals, reptiles and amphibians, fish, and of worms [40],

[41], [42], [23], [3], [4]. Torrent-Guasp's model of the helical heart includes the cardiac structures that produce two simple loops that start at the pulmonary artery and end in the aorta, unraveling the Gordian knot of the architectural arrangement of ventricular muscle mass [40]. Figure 8 left shows the unfolding of the heart into a helical structure. For Torrent-Guasp the simplest model of a heart is a rope closing in two rotations [40], [41]. It is thus also a GML_m^n body ($m = 1/2$ closing in two rotations, hence a $1/2$ -angle). The rope model and the $\frac{1}{2}$ angle have constant cross-section along the path, but this can change along the path in Equation (2.1). The relation of the helical heart and Generalized Möbius-Listing surfaces and bodies was suggested by Dr. Mamanthi Rogava [28].

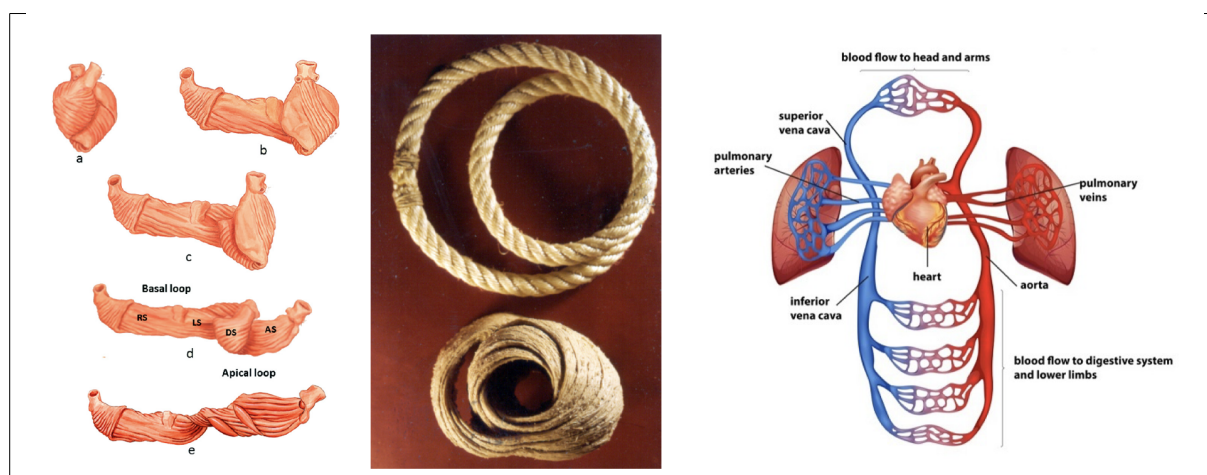


FIGURE 8. Left: unraveling of the heart. Center: Rope model of the heart. Right: Overview of the circulatory system

We propose that the whole circulatory system, with the heart as central organ, can be considered as a single system. The whole system then is a single GML body (with annular cross-section), whereby the aorta and the vena cava have a (approximately) circular cross section. From the analytic definition, in particular the twisting parameter in Equation (2.1) a GML surface or body can either exhibit a cylinder phenomenon or a Möbius phenomenon. A question is whether a system exists that can switch between both states. Here the Torrent-Guasp model provides a clue, in the sense that the motion of the heart is spiral, with a twist [40], [3]. In this way, the heart has two states, in which the two $S_{0-Aorta}$ and $S_{0-VenaCava}$ have a relative orientation to each other. Assuming that the positions can switch because of the continuous twisting and untwisting of the structure [40], we have:

Proposition 7.1. *If two sections suffice ($S_{0-Aorta}$ and $S_{0-VenaCava}$) in GML , and the motion of the helical heart is a twist rotation, alternate switching between two-sided (Cylinder) and one-sided (Möbius), then the function can switch from Transport (Cylinder) to Exchange (Möbius).*

Remark 7.2. Simply twisting a GML body with annular cross section does not create a Möbius phenomenon of the structure, but it occurs both on the outer and inner surfaces. By separating zones in the blood stream, certain zones can achieve the Möbius phenomenon. See Remark 4.1.

Remark 7.3. Our proposition focuses in first instance on the spiral movements of the Torrent-Guasp model [25], but Dr. Rogava considers three different movements of the heart, including the displacement of the center of gravity. For this he considers the Möbius-Listing-Tavkhelidze three-dimensional body winding principle, as a better model [27].

Our models focus not only on shape and geometry, but also on transport of physical entities or energy, and on exchange between very different structures. It is contemplated that the geometric models as described for the circulatory systems, using Generalized Twisting and Rotating Bodies (*GTR*), Generalized Möbius Listing surfaces and bodies (*GML*), and Gielis transformations [8] can be extended to include systems in biology, botany, ecology, physics (e.g., open and closed thermodynamic systems) and even spacetimes [10].

REFERENCES

- [1] K. Arslan, B. Bulca, B. Bayram, G. Ozturk and H. Ugail, *On spherical product surfaces in E^3* , International Conference on CyberWorlds (2009), 132-137. IEEE.
- [2] N.H. Bishopric, *Evolution of the heart from bacteria to man*. Annals of the New York Academy of Sciences **1047(1)** (2005),13-29. DOI 10.1196/annals.1341.002
- [3] G.D. Buckberg, *Basic science review: the helix and the heart*, The Journal of Thoracic and Cardiovascular Surgery **124(5)** (2002), 863-883. DOI 10.1067/mtc.2002.122439
- [4] G.D. Buckberg, *Rethinking the cardiac helix—a structure/function journey: overview*. European Journal of Cardio-Thoracic Surgery **29** (2006).
- [5] B. Bulca, K. Arslan, B. Bayram and G. Öztürk, *Canal surfaces in 4-dimensional Euclidean space*, International Journal of Optimization and Control: Theories & Applications (IJOCTA) **7(1)** (2017), 83-89. DOI 10.11121/ijocta.01.2017.00338
- [6] D. Caratelli, J. Gielis, P. E. Ricci and I. Tavkhelidze, *Some properties of "bulky" links generated by generalized Mobius-Listing's bodies GML_4^n* , Journal of Mathematical Sciences **216(4)** (2016). DOI 10.1007/s10958-016-2907-x
- [7] Y. Fougerolle, F. Truchetet and J. Gielis, *Potential fields of self intersecting Gielis curves for modeling and generalized blending techniques*, In: Modeling in Mathematics: Proceedings of the Second Tbilisi-Salerno Workshop on Modeling in Mathematics, Atlantis Press, 2017, pp. 67-81. DOI 10.2991/978-94-6239-261-8-6
- [8] J. Gielis, *A generic geometric transformation that unifies a wide range of natural and abstract shapes*, American Journal of Botany, **90(3)** (2003), 333-338. DOI 10.3732/ajb.90.3.333
- [9] J. Gielis and R. Grigolia, *Lamé curves and Rvachev's R-functions*, Reports of enlarged sessions of the Seminar of I. Vekua Institute of Applied Mathematics-Tbilisi **37** (2022), 1-4.
- [10] J. Gielis, S. Haesen and L. Verstraelen, *Universal natural shapes: From the super eggs of Piet Hein to the cosmic egg of Georges Lemaitre*, Kragujevac Journal of Mathematics **28** (2005), 57-68.
- [11] J. Gielis, P. Shi, B. Beirinckx, D. Caratelli and P.E. Ricci, *Lamé-Gielis curves in biology and geometry*, Proceedings of the Conference Riemannian Geometry and Applications RIGA 2021 (Mihai I., Mihai A. Eds.).
- [12] J. Gielis and I. Tavkhelidze, *The general case of cutting of Generalized Möbius-Listing surfaces and bodies*, 4Open **3(7)** (2020). DOI 10.1051/fopen/2020007
- [13] J. Gielis and I. Tavkhelidze, *The Möbius phenomenon in generalized Möbius-Listing bodies with cross sections of odd and even polygons*. Growth and Form **2(1)** (2022), 1-10
- [14] J. Gielis and I. Tavkhelidze, *A Note on generalized Möbius-Listing bodies*, In: Athena Transactions in Mathematical and Physical Sciences **1**, Proceedings of the 1st International Symposium on Square Bamboos and the Geometree, 2023.
- [15] J. Gielis, I. Tavkhelidze and P. E. Ricci, *About bulky links, generated by generalized Mobius-Listing's bodies GML_2^n* , Journal of Mathematical Sciences **193(3)** (2013). DOI 10.1007/s10958-013-1474-7
- [16] J. Gielis, I. Tavkhelidze and P.E. Ricci, *The Möbius phenomenon in Generalized Möbius-Listing surfaces and bodies, and Arnold's Cat phenomenon*, Advanced Studies, Euro-Tbilisi Mathematical Journal **14(4)** (2021), 17-35. DOI 0.32513/asetmj/1932200812

- [17] W. Goemans and I. Van de Woestyne, *Clelia curves, twisted surfaces and Plücker's conoid in Euclidean and Minkowski 3-space*, Recent Advances in the Geometry of Submanifolds: Dedicated to the Memory of Franki Dillen **674** (2016), 59. DOI 10.7326/0003-4819-59-5-674
- [18] R. Grigolia, *Three-valued Gödel Logic with Constant and Involution for Application to R-functions*. In: Athena Transactions in Mathematical and Physical Sciences, Volume 1. Proceedings of the 1st International Symposium on Square Bamboos and the Geometree (2023)
- [19] G. Gündüz, *Physics in deformable spacetime: Physical laws emerging from the surface minimality principle and the masses of particles*, Results in Physics (2023). DOI 10.1016/j.rinp.2023.106981
- [20] D.S. Hall, M.W. Ray, K. Tiurev, E. Ruokokoski, A.H. Gheorghe and M. Möttönen, *Tying Quantum Knots*. Nature Physics, DOI:10.1038/NPHYS3624
- [21] R. Herges, *Topology in chemistry: designing Möbius molecules*, Chemical Reviews **106(12)** (2006), 4820-4842. DOI 10.1021/cr0505425
- [22] B. Jensen, T. Wang, V.M. Christoffels and A.F. Moorman, *Evolution and development of the building plan of the vertebrate heart*, Biochimica et Biophysica Acta (BBA)-Molecular Cell Research **1833(4)** (2013), 783-794.
- [23] M.J. Kocica, A.F. Corno, F. Carreras-Costa, M. Ballester-Rodes, M.C. Moghbel, C.N Cueva and F. Torrent-Guasp, *The helical ventricular myocardial band: global, three-dimensional, functional architecture of the ventricular myocardium*, European Journal of Cardio-Thoracic Surgery **29**(Supplement) (2006). DOI 10.1016/j.ejcts.2006.03.011
- [24] M. Matsuura, *Gielis' superformula and regular polygons*, Journal of Geometry **106** (2015), 383-403. DOI /10.1007/s00022-015-0269-z
- [25] A. Nasiraei-Moghaddam and M. Gharib, *Evidence for the existence of a functional helical myocardial*, American Journal of Physiology-Heart and Circulatory Physiology **296(1)** (2009), H127-H131. DOI 10.1152/ajpheart.00581.2008
- [26] R. Penrose, *Fashion, Faith and Fantasy in the New Physics of the Universe*, Princeton University Press, 2016. DOI 10.1515/9781400880287
- [27] M. Rogava, *About the issues of the perfect modeling of the heart*, (in Georgian, with English abstract), Cardiology And Internal Medicine XXI - Achievements and Problems **1-4** (LXX- LXXIV) Tbilisi (2019-20), 54-88.
- [28] M. Rogava and I. Tavkheldidze, *The algorithm of changes in systolic-diastolic motion in relation to heart's center of gravity in norm and pathology* (in Georgian), Cardiology and Internal Medicine XXI **1-4** (2013), 27-30.
- [29] V.L. Rvachev, *Geometric Applications of Logic Algebra*, Naukova Dunka, 1967 (in Russian).
- [30] G.R. Schaller and R. Herges, *Möbius molecules with twists and writhes*. Chemical Communications **49(13)** (2013), 1254-1260. DOI 10.1039/C2CC34763F
- [31] I. Tavkheldidze, *On the some properties of one class of geometrical figures and lines*, Reports of Enlarged Sessions of the Seminar of I. Vekua Institute of Applied Mathematics **16(1)** (2001), 35-38.
- [32] I. Tavkheldidze, *About connection of the generalized Möbius-Listing's surfaces with sets of ribbon knots*, Proceedings of Ukrainian Mathematical Congress S. 2, Topology and Geometry-Kiev, 2011, 117-129.
- [33] I. Tavkheldidze, *About some properties of one special class of the Generalized Möbius-Listing bodies*, Reports of enlarged sessions of the Seminar of I. Vekua Institute of Applied Mathematics-Tbilisi **36** (2022), 91-96.
- [34] I. Tavkheldidze, *Geometric figures which appear after VV Cutting in the radial Cross Section of Generalized Möbius-Listing bodies*, In: Athena Transactions in Mathematical and Physical Sciences **1**, Proceedings of the 1st International Symposium on Square Bamboos and the Geometree (ISSBG), 2023.
- [35] I. Tavkheldidze, D. Caratelli, J. Gielis, J., P.E. Ricci, M. Rogava and M. Transirico, *On a geometric model of bodies with "Complex" configuration and some movements*, Modeling in Mathematics (2017), 129-158. Atlantis Press, Paris. DOI10.2991/978-94-6239-261-8-10

- [36] I. Tavkheldidze, C. Cassisa, J. Gielis and P.E. Ricci, *About bulky links, generated by generalized Möbius-Listing's bodies GML_3^n* , Rendic. Lincei Mat. Appl. **24** (2013), 11-38. DOI 10.471/RLM/643
- [37] I. Tavkheldidze, C. Cassisa and P.E. Ricci, *About connection of the generalized Möbius-Listing's surfaces with sets of knots and links*, Lecture Notes of Seminario Interdisciplinare di Matematica **9** (2010), 187-200.
- [38] I. Tavkheldidze and J. Gielis, *Geometric figures which appear after VS cutting in the radial cross section of generalized Möbius-Listing bodies*, Reports of Enlarged Sessions of the Seminar of I. Vekua Institute of Applied Mathematics **37**, 2023.
- [39] I. Tavkheldidze and P.E. Ricci, *Some properties of "bulky" links, generated by generalised Möbius-Listing's bodies*, in: Modeling in Mathematics, Atlantis Press, Paris, PE (2017), 159–185. DOI 10.2991/978-94-6239-261-811
- [40] F. Torrent-Guasp, *Estructura macroscópica del miocardio ventricular*, Rev. Esp. Cardiol. **33(3)** (1980), 265-87.
- [41] F. Torrent-Guasp, G.D. Buckberg, C. Clemente, J.L. Cox, H.C. Coghlan and M. Gharib, *The structure and function of the helical heart and its buttress wrapping. I. The normal macroscopic structure of the heart*. In Seminars in Thoracic and Cardiovascular Surgery, WB Saunders **13(4)** (2001), 301-319. DOI 10.1053/stcs.2001.29953
- [42] F. Torrent-Guasp, M.J. Kocica, A.F. Corno, M. Komeda, F. Carreras-Costa, A. Flotats and H. Wen, *Towards new understanding of the heart structure and function*, European Journal of Cardio-Thoracic Surgery **27(2)** (2005), 191-201. DOI 10.1016/j.ejcts.2004.11.026
- [43] G.B. West, J.H. Brown and B.J. Enquist, *A general model for the origin of allometric scaling laws in biology*, Science **276(5309)** (1997), 122-126. DOI 10.1126/science.276.5309.122

DEPARTMENT OF BIOSCIENCES ENGINEERING, UNIVERSITY OF ANTWERP, BELGIUM

Email address: johan.gielis@gmail.com

DEPARTMENT OF MATHEMATICS, TBILISI, TBILISI STATE UNIVERSITY, TBILISI, GEORGIA

Email address: ilia.tavkheldidze@tsu.ge

SECT. OF MATHEMATICS, INTERNATIONAL TELEMATIC UNIVERSITY UNINETTUNO, ROMA, ITALIA

Email address: paoloemilioricci@gmail.com